Structure−Function Analysis of a Phage Display-Derived Peptide That Binds to Insulin-like Growth Factor Binding Protein 1‡

Nicholas J. Skelton,*,§ Yvonne M. Chen,§ Nathan Dubree,|| Clifford Quan,|| David Y. Jackson,|| Andrea Cochran,§ Kerry Zobel,§ Kurt Deshayes,§ Manuel Baca,§ M. Teresa Pisabarro,§ and Henry B. Lowman§

Departments of Protein Engineering and Bioorganic Chemistry, Genentech, Inc., 1 DNA Way, South San Francisco, California 94080

Received February 23, 2001; Revised Manuscript Received May 18, 2001

ABSTRACT: Highly structured, peptide antagonists of the interaction between insulin-like growth factor 1 (IGF-I) and IGF binding protein 1 (IGFBP-1) have recently been discovered by phage display of naïve peptide libraries [Lowman, H. B., et al. (1998) *Biochemistry 37,* 8870−8878]. We now report a detailed analysis of the features of this turn−helix peptide motif that are necessary for IGFBP-1 binding and structural integrity. Further rounds of phage randomization indicate the importance of residues contributing to a hydrophobic patch on one face of the helix. Alanine-scanning substitutions confirm that the hydrophobic residues are necessary for binding. However, structural analysis by NMR spectroscopy indicates that some of these analogues are less well folded. Structured, high-affinity analogues that lack the disulfide bond were prepared by introducing a covalent constraint between side chains at positions *i* and $i + 7$ or $i + 8$ within the helix. Analogues based on this scaffold demonstrate that a helical conformation is present in the bound state, and that hydrophobic side chains in this helix, and residues immediately preceding it, interact with IGFBP-1. By comparison of alanine scanning data for IGF-I and the turn−helix peptide, we propose a model for common surface features of these molecules that recognize IGFBP-1.

Phage display has emerged as a powerful technique for discovery and optimization of peptide ligands to proteins of biological interest (reviewed in ref *1*). The combination of phenotype (the displayed peptide) and genotype (the DNA sequence encoding the peptide) within the phage particle allows efficient sorting and amplification of libraries containing on the order of $10^{10}-10^{12}$ individual members (*2*). So-called "naïve" peptide libraries, in which peptides of 15−20 residues of random sequence are fused via a flexible linker to gene III or gene VIII coat protein of M13 phage, have led to the discovery of novel, structurally defined antagonists and agonists of protein−protein interactions (see, for example, refs *3*−*5*). Inclusion of potential conformational restraints (e.g., pairs of cysteine residues to form disulfide bonds) improves the recovery of high-affinity peptides during the selection process, presumably by imparting structural bias to the peptide (thereby reducing the entropic cost of binding to the target) (*1*, *6*). The phage display process selects primarily for binding, sometimes modulated by avidity, expression, secretion, or stability effects. However, structural analysis of a number of these peptides, either free in solution (*5*, *7*) or in complex with their target protein (*3*, *4*, *7*−*11*), indicates that they often adopt compact conformations and may be considered miniprotein domains. Thus, the phage optimization process may also select for these stable, structural motifs in some instances.

The ability of phage display to identify new molecules that influence protein−protein interactions has great promise for developing novel biotechnology reagents, e.g., by blocking a particular protein−protein interaction and thereby validating it as a suitable drug target or for selectively antagonizing particular elements of a complex, multicomponent signaling pathway to allow a better understanding of function. Although phage display can identify peptides of potent and selective activity in vitro, peptides are not usually considered good drug candidates because of poor bioavailability following oral administration and rapid clearance or degradation when injected into the serum. However, phage-derived peptides bind tightly and selectively to their target; hence, they may provide useful starting points from which drug-like molecules might be designed. While those peptide side chains that contribute to protein binding can be established from affinity measurements for peptide analogues, the spatial relationship between the moieties necessary for binding is best established from structural studies of the peptide bound to its target protein (*3*, *4*, *7*−*10*). With this information in hand, the process of design, synthesis, and screening of small molecules presenting the pharmacophore can begin.

IGF-I[1] plays a crucial role in cell growth and metabolism because of its ability to bind and activate cell surface receptors [IGF receptor 1 and the insulin receptor (*12*)]; in vivo, this process is modulated by six binding proteins

‡ Atomic coordinates have been deposited in the Protein Data Bank for three of the peptides described in this work for which three-dimensional structures were determined. Accession numbers for minimized mean and ensembles are 1gje and 1imw for bp1-01, 1gjf and 1in2 for bp1($i + 7$)C, and 1gjg and 1in3 for bp1($i + 8$)D, respectively.

* To whom correspondence should be addressed. Telephone: (650) 225-6402. Fax: (650) 225-3734. E-mail: skelly@gene.com.

§ Department of Protein Engineering.

|| Department of Bioorganic Chemistry.

10.1021/bi0103866 CCC: $20.00
Published on Web 06/29/2001

(IGFBP-1−6) that sequester the hormone and prevent receptor binding (*13*). Control of the IGF receptor signaling pathway may provide an efficient means of affecting metabolic diseases such as diabetes (*14*). Antagonists of the interaction between IGF-I and IGFBP-1 hold promise in this regard since they would block sequestration of the endogenous IGF-I, raise local concentrations of the hormone, and promote signaling. Recently, a series of phage-derived peptides have been described that block binding of IGF-I to IGFBP-1 (*5*). One such 15-residue peptide, termed bp1-01, binds to IGFBP-1 with a K_d of ~1 μM. Analysis of NMR data indicates that this peptide adopts a stable turn−helix fold in solution. The phage-derived peptides have been shown to promote IGF-I signaling activity in the context of an in vitro KIRA assay (*5*), and hence may constitute a good starting point for the design of small molecules having therapeutic potential.

To date, only limited structural information has been reported for any IGF binding protein (*15*), and we have been unsuccessful in our attempts to characterize structurally the complex between the phage peptides and IGFBP-1. To learn what features of the peptide are necessary for binding to IGFBP-1, we now report a detailed structure−activity analysis based on the conformation of the uncomplexed peptide in solution. Transfer of the epitope identified in this work to a more rigid peptide scaffold produces molecules that still bind tightly to IGFBP-1, demonstrating that the conformation of the peptide free in solution is similar to that present when bound to IGFBP-1. Finally, by considering structure−activity data for IGF-I itself (*16*), we hypothesize about the surface regions of IGF-I that the peptides mimic when they bind to IGFBP-1.

MATERIALS AND METHODS

Polyvalent bp1-02 Peptide−Phage Binding Selections. A phagemid clone, Φ1 (*5*), containing DNA encoding the bp1-02 peptide, SEVGCRAGPLQWLCEKYFG, fused through a linker peptide, GGSGGGA, to the N-terminus of the bacteriophage M13 major coat protein gene, gVIII, was used as the starting point for further peptide mutagenesis. Note that throughout this work, peptide residues are numbered with the N-terminal cysteine as residue 1 since in all of the subsequent synthetic peptides, the four N-terminal residues of bp1-02 were omitted. Templates with TAA stop codons at the sites targeted for randomization were prepared to prevent contamination by the wild-type sequence. Degenerate NNS codons (where N is an equal mixture of A, G, C, and T and S is an equal mixture of G and C) were used in standard mutagenesis reactions (*17*) to generate four libraries in which the following residues were randomized: Gly4, Pro5, Leu6, and Trp8 (library 1); Arg2, Gln7, Leu9, and Glu11 (library 2); Ala3, Lys12, and Tyr13 (library 3); and Gly−1, Glu11, Lys12, Tyr13, and Phe14 (library 4). The products of random mutagenesis reactions were electroporated into *Escherichia coli* strain SS-320 (*2*) and amplified at 37 °C overnight with M13K07 helper phage (Stratagene). After incubation at 37 °C for 1 h, estimates of 2×10^7 to 1×10^8 transformants per library were obtained by titration.

Human IGFBP-1 was produced in Chinese hamster ovary cells (*18*) as previously described (*5*). To minimize avidity effects, phage were equilibrated with biotinylated IGFBP-1 in solution. Typically, 10^9-10^{10} purified phage were treated with MPBST (PBS containing 5% skim milk and 0.05% Tween-20) for 1 h at room temperature and equilibrated with the biotinylated target at room temperature for 1 h (rounds 1−3) or overnight (round 4). The concentration of the target was reduced in successive rounds of selection (400, 200, 20, and 4 nM for rounds 1−4, respectively). Target-bound phage were captured by incubating with streptavidin magnetic beads (Promega) for 2−5 min at room temperature. The beads were then washed up to 10 times with PBS-Tween or MPBST before eluting bound phage with 0.1 M HCl and immediately neutralizing with $^1/_3$ volume of 1 M Tris (pH 8.0). The eluted phage were propagated by infecting XL-1 *E. coli* cells (Stratagene) for the next selection cycle. After four rounds of selection, 40, 61, 93, and 66 clones were sequenced for libraries 1−4, respectively.

BIAcore Kinetics Assays. The affinity of bp1-02 for IGFBP-1 was determined in direct binding assays in which the association and dissociation kinetics were measured using a BIAcore-2000 (BIAcore, Inc., Piscataway, NJ) SPR instrument (*19*). IGFBP-1 was covalently coupled onto carboxymethyl dextran biosensor chips (CM-5; BIAcore, Inc.) via EDC and NHS, as described by the manufacturer, to a density of ~2700 RU. Unreacted groups were blocked by reaction with 1 M ethanolamine. For kinetics measurements, serial dilutions of peptide were injected in running buffer (phosphate-buffered saline, containing 0.1% Tween-20 and 0.01% sodium azide) at a flow rate of 10 μL/min for 3 min, followed by a dissociation period of 5 min (see Figure 2A). No regeneration step was used, as the peptide had fully dissociated by the end of the dissociation period as judged by a return of the SPR signal to baseline. Association (k_{on}) and dissociation (k_{off}) rates were determined from a fit of the data to a 1:1 Langmuir binding model using the manufacturer's analysis software.

BIAcore Inhibition Assays. The ability of bp1-01 peptide variants to inhibit IGFBP-1 binding to IGF-1 was assessed in a competitive binding assay using the BIAcore-2000 instrument. This type of assay has previously been used to compare the relative affinities of IGF-1 variants for binding to the IGF binding proteins (*20*). IGF-1 was biotinylated as previously described (*5*) and captured by injection over a streptavidin-linked biosensor chip (SA chip; BIAcore, Inc.) at a density of 400−800 RU. Serial dilutions of each bp1-01 variant, in addition to a wild-type control, were mixed with a constant concentration (40 nM) of IGFBP-1 in running buffer containing 0.05% ovalbumin (Sigma) to prevent nonspecific binding. In some cases, 1−2.5% DMSO was added to prevent peptide precipitation. After incubation for ≥1 h at room temperature, 30 μL samples were injected at a flow rate of 10 μL/min over an IGF-1-coated flow cell as

[1] Abbreviations: 2QF-COSY, double-quantum-filtered spectroscopy; DCM, dichloromethane; DIPEA, diisopropylethylamine; DMA, *N*,*N*-dimethylacetamide; DMSO, dimethyl sulfoxide; EDC, *N*-ethyl-*N*′-[3-(dimethylamino)propyl]carbodiimide hydrochloride; FMOC, 9-fluorenylmethyloxycarbonyl; HATU, *O*-(7-azabenzotriazol-1-yl)-*N*,*N*,*N*′,*N*′-tetramethyluronium hexafluorophosphate; HBTU, 2-(H-benzotriazol-1-yl)-1,1,3,3-tetramethyluronium hexafluorophosphate; IGF-I, insulin-like growth factor I; IGFBP, IGF binding protein; KIRA, kinase receptor activation; NHS, *N*-hydroxysuccinimide; NMR, nuclear magnetic resonance; NOESY, nuclear Overhauser effect spectroscopy; rms, root-mean-square; ROESY, rotating frame Overhauser effect spectroscopy; RU, response units; SPR, surface plasmon resonance; TOCSY, total correlation spectroscopy.

well as over a control (streptavidin only) flow cell. After each injection, the signal from the control flow cell was subtracted, and then the relative amount of IGFBP-1 bound to IGF-1 was recorded as the net response over pre-injection baseline. Regeneration was achieved with a 30 s pulse of 10 mM HCl. The amount of free IGFBP-1 was plotted as a function of peptide concentration and fit to a four-parameter binding curve (*21*) using the program KaleidaGraph (Synergy Software) (see Figure 2B). Relative activities were calculated as the IC_{50}(variant)/IC_{50}(wt) ratio.

Peptide Synthesis. All peptides were synthesized as C-terminal amides on a Pioneer synthesizer (PE Biosystems) using standard solid phase peptide chemistry with FMOC-protected amino acids on a *p*-alkoxybenzyl alcohol resin. Amino acids were purchased from BACHEM Ca. (Advanced ChemTech) or Calbiochem Corp. Amide couplings were performed with 2−4 equiv of HBTU-activated amino acid and 4 equiv of *N*-methylmorpholine. FMOC groups were removed with 20% piperidine in DMA. Cleavage and deprotection with TFA containing 5% triethylsilane afforded crude linear peptides after evaporation of the TFA. The resin was washed with diethyl ether, and the peptide were extracted from the resin with 100 mL of a 2:1 water/acetonitrile mixture. Disulfide oxidation was carried out via dropwise addition of a saturated solution of iodine in acetic acid at 25 °C with vigorous stirring until a slight yellow color persisted. In some cases, peptides were purified by HPLC before and after formation of the cyclic disulfides. The oxidized peptides were lyophilized and purified by preparative reverse phase C-18 HPLC (CH_3CN/H_2O gradient, 0.1% TFA). Pure fractions (>98% pure as determined by analytical HPLC) were combined and characterized by electrospray ionization mass spectrometry (Sciex API100) and lyophilized.

The locked-helix peptides were synthesized by a modified version of the previously published procedure (*22*). Peptides were synthesized as described above, with coupling of FMOC-Glu(OAll)-OH (Nova Biochem) at the C-terminal position of the "lock". The 1,5-diaminopentane linker was precoupled to the side chain of the second Glu and incorporated into the peptide (at the more N-terminal position of the lock) as the FMOC-Glu-(5-*N*-Alloc-1,5-diaminopentyl) amide (the FMOC amino acid was a gift from A. Braisted). After acetylation of the N-terminus, allyl protecting groups were removed by treatment for 1.5 h with dichlorobis-(triphenylphosphine)palladium(II) (100 mg per 0.2 mequiv of resin) dissolved in 10% piperidine in DMA. The resin was then washed successively with 20% piperidine in DMA, DMA, a solution of sodium diethyldithiocarbamate trihydrate (100 mg) and 10% DIPEA in DMA, DMA, and DCM. The resin was resuspended in dichloromethane. After addition of DIPEA (1.5 mmol/mequiv of resin), the deprotected side chains were coupled by dropwise addition of HATU (1 mmol/mequiv of resin) dissolved in a minimum volume of DMA. After 1.5−3 h, the resin was washed and tested with ninhydrin for free amines. If cyclization was not complete, the resin was treated again with 0.5 equiv of HATU. Cleavage and purification were as described above.

NMR Spectroscopy and Structure Calculations. NMR samples contained 5−10 mM peptide in a 92% H_2O/8% D_2O mixture (pH 5.0−5.3) and ∼100 μM 1,4-dioxane as a chemical shift reference. All spectra were acquired on a Bruker DRX-500 spectrometer at 30 °C as described previously (*5*, *23*). Distance restraints and dihedral angle restraints were generated from ROESY data (τ_m = 150 ms) and 2QF-COSY or COSY-35 spectra, respectively, as described in ref *24*. One hundred initial structures were calculated using the hybrid distance geometry/simulated annealing program DGII (*25*); 80 of these were further refined by restrained molecular dynamics using the AMBER all atom force field implemented in DISCOVER as described previously (*24*). Twenty conformations of lowest restraint violation energy were chosen to represent the solution conformations. In no structure were there any distance restraint violations of >0.1 Å, any dihedral angle restrain violations of >1.5°, or any residue with backbone geometry in a disallowed region of $\phi-\psi$ space. A summary of input restraints and structural statistics for the three calculated structures is presented in Table 1 of the Supporting Information.

RESULTS

Conservation of Residues in Secondary Phage Libraries. Previously, we reported a 19-residue peptide that binds to IGFBP-1 (bp1-02). This peptide, and the truncated analogue bp1-01, inhibit the binding of IGF-I to IGFBP-1 with IC_{50} values in the low micromolar range (*5*). In the study presented here, polyvalent phage display on gVIII has been used to identify those residues that are critical for IGFBP-1 binding. Nucleotides corresponding to all non-cysteine residues within bp1-02 were randomized in at least one of four phage libraries (see Materials and Methods), and the libraries were subjected to four rounds of selection against IGFBP-1 and amplification. In subsequent sequencing of the selected phage clones, residues were assigned to one of three categories depending on whether the original amino acid type was (i) always, (ii) mostly, or (iii) rarely the same as that observed in the original bp1-02 peptide (Figure 1A and Table 2 of the Supporting Information). Leu6, Trp8, and Leu9 fall into the first category, while Gly4, Pro5, Tyr13, and Phe14 fall into the second category. The highly conserved nature of these side chains suggests that they are more important for IGFBP-1 binding than the less conserved class iii side chains.

Measurement of Peptide Affinity for IGFBP-1. We used surface plasmon resonance (BIAcore) to characterize the binding of peptides to immobilized IGFBP-1. The dissociation of bp1-01 was too fast for accurate determination of the off-rate. Dissociation of the longer variant bp1-02 was slower (Figure 2A), and the rate constants could be measured (k_{on} = 2.30 × 10^5 M^{-1} s^{-1}; k_{off} = 5.03 × 10^{-2} s^{-1}; K_d = 0.22 μM). The dissociation rate constant indicates a half-life for the peptide−IGFBP-1 complex of 28 s. The association rate constant is moderately fast, consistent with the notion that the peptide does not undergo a significant conformational change upon binding to IGFBP-1.

Many of the peptides discussed below had binding kinetics similar to those of bp1-01 (i.e., dissociation rate too fast to characterize accurately). Instead, a competitive binding assay using BIAcore detection was used to measure the ability of these peptides to inhibit the binding of IGFBP-1 to biotinylated IGF-I presented on streptavidin-coated biosensor chips. In these assays, an IC_{50} of 1 or 0.2 μM was observed for inhibition by bp1-01 or bp1-02, respectively (Figure 2B). We find that the BIAcore competition assay gives more

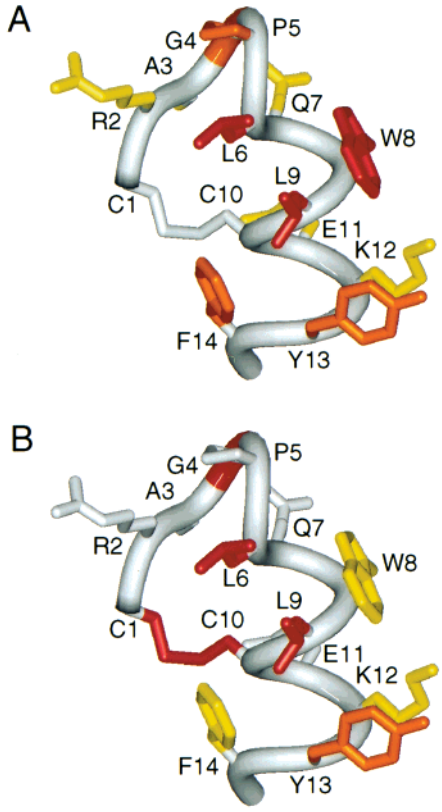

FIGURE 1: (A) Residue conservation during phage optimization of bp1-01. Side chains on the bp1-01 minimized mean structure (*5*) are colored red, orange, or yellow, for residues that are always, mostly, or not conserved, respectively. (B) Inhibition of IGF-I binding to IGFBP-1 by alanine-scan analogues. The side chains of the minimized mean bp1-01 structure (*5*) are colored according to the effect on IC_{50} relative to bp1-01: white (1−2-fold), yellow (2−10-fold), orange (10−30-fold), or red (>30-fold). This figure was prepared using the program InsightII (MSI, San Diego).

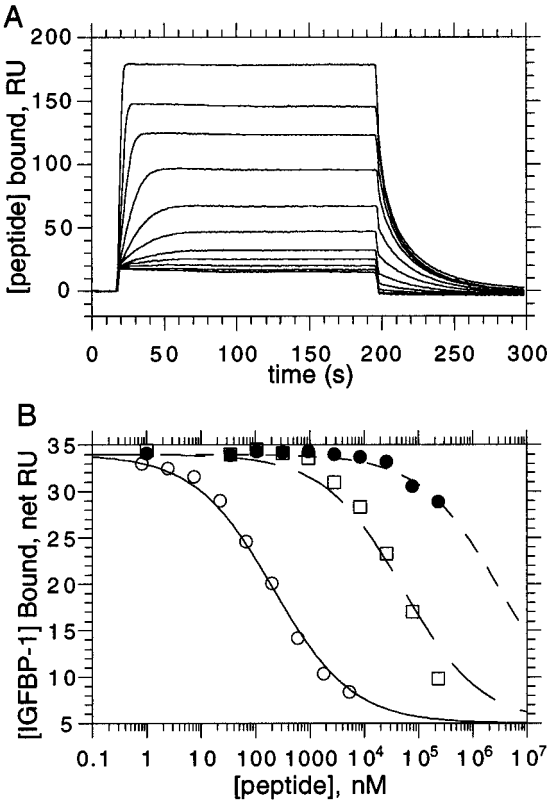

FIGURE 2: (A) Association and dissociation kinetics of peptide bp1-02 using the BIAcore instrument. Serial dilutions of peptide from 3.3 μM to 1.3 nM were injected over IGFBP-1 immobilized on a carboxymethyl dextran biosensor chip. Bound peptide is shown as response units (RU) as a function of time. (B) Inhibition assays using the BIAcore instrument for detection of free IGFBP-1. Serial dilutions of peptides bp1-01 (○), bp1-04 (●), or bp1(i + 7)D (□) were mixed with IGFBP-1 and injected over a streptavidin chip to which biotinylated IGF-1 was bound. The relative amount of IGFBP-1 binding to IGF-1 was measured immediately after injection of each sample and plotted as a function of peptide concentration. Four-parameter fits were used to calculate IC_{50} values (see Materials and Methods).

reproducible results than the ELISA competition that we have used previously (*5*, *16*). For a number of peptides, the level of inhibition of binding was also measured with an IGF-I phage ELISA (data not shown); IC_{50} values determined with this method were comparable to those obtained with the BIAcore instrument.

Scanning Mutagenesis of bp1-01 Using Synthetic Peptides. To assess directly the importance of each side chain, we replaced each residue individually with alanine. BIAcore competition experiments were performed with each variant to assess the degree of inhibition (IC_{50}) of binding between IGFBP-1 and IGF-I (Table 1). Side chains that were conserved or mostly conserved in the phage analysis generally also caused a greater than 6-fold increase in IC_{50} when substituted with alanine (Figure 1B). Pro5 is the only exception to this; it was mostly conserved, but alanine substitution increased IC_{50} only 1.5-fold.

NMR spectroscopy was used to assess the impact of the alanine substitutions on the structure of the peptides. Replacement of both cysteine residues of bp1-01 with serine produced a low-affinity peptide whose NMR parameters indicate the absence of folded structure (*5*). Thus, the analogue lacking the disulfide bond is a good model for the unfolded state, and deviations of $^3J_{HN-H\alpha}$ coupling constants and H^α chemical shifts from the values observed in this analogue give an indication of the extent to which other analogues are folded. The rms differences for these parameters are listed in Table 1, and are maximal for bp1-01 [1.63 Hz and 0.25 ppm for $^3J_{HN-H\alpha}$ and $\delta(H^\alpha)$, respectively]. The alanine analogues form a continuum between the folded (bp1-01) and unfolded (Cys to Ser analogue) state, with replacement of Gly4, Leu6, or Leu9 having a large destabilizing effect, removal of the aromatic rings having a moderate effect, and other analogues being close to fully folded. For the less folded analogues (as judged from the NMR parameters), loss of affinity may in part be due to the structural reorganization and not to the loss of direct IGFBP-1 contacts.

Additional Single-Residue Substitutions. A number of other analogues were synthesized to obtain a more complete structure−activity relationship for bp1-01, as summarized in Table 2. These analogues focus on three areas of the bp1-01 structure: the Gly-Pro turn preceding the helix, the pair of leucines in the middle of the helix, and the aromatic residues at the C-terminus of the helix.

In the ensemble of structures determined for bp1-01, Gly4 has a ϕ angle that is either positive or close to 180°. Placing an L-amino acid in such a conformation would be energetically unfavorable, because of both intrinsic backbone con-

Table 1: Relative Activities and Structural Integrity of bp1-01 Ala-Scan Peptide Variants

	name	relative activity[a] IC_{50}(mut)/IC_{50}(wt)	$^3J_{HN-H\alpha}$[b] (Hz)	$\delta(H^\alpha)$[c] (ppm)
wild type	bp1-01	1.0	1.65	0.28
Cys1Ser, Cys2Ser	bp1-06	220	0.0	0.0
Arg2Ala	bp1-115	0.9	nd	nd
Gly4Ala	bp1-29	50	0.56[d]	0.10[d]
Pro5Ala	bp1-30	1.5	nd	nd
Leu6Ala	bp1-72	30	0.77	0.10
Gln7Ala	bp1-71	0.7	1.71	0.18
Trp8Ala	bp1-70	7.4	1.35	0.16
Leu9Ala	bp1-69	33	0.81	0.09
Glu11Ala	bp1-76	2.9	1.17	0.13
Lys12Ala	bp1-75	3.4	1.46[e]	0.19[e]
Tyr13Ala	bp1-74	13	1.31	0.15
Phe14Ala	bp1-73	6.2	1.37	0.15

[a] Relative inhibitory activities were determined from the IC_{50} for inhibition of IGFBP-1 binding to immobilized IGF-I in BIAcore competition assays; the inhibition by the analogue peptide [IC_{50}(mut)] is compared to the inhibition by bp1-01 [IC_{50}(wt) = 1.1 ± 0.7 μM]. [b] The rms differences of $^3J_{HN-H\alpha}$ between the analogue listed at the left and the unfolded cysteine to serine analogue (bp1-06). NMR data were not analyzed for the analogues indicated by nd. [c] The rms differences in the H^α chemical shift between the analogue listed at the left and the unfolded cysteine to serine analogue (bp1-06). NMR data were not analyzed for the analogues indicated by nd. [d] Values calculated for the predominant trans form of the Ala−Pro peptide bond. [e] NMR data collected in 16% (v/v) acetonitrile to limit self-association of this peptide.

Table 2: Relative Activities and Structural Integrity of bp1-01 Peptide Variants

analogue[a]	name	relative activity[b] IC_{50}(mut)/IC_{50}(wt)	$^3J_{HN-H\alpha}$[c] (Hz)	$\delta(H^\alpha)$[d] (ppm)
wild type	bp1-01	1.0	1.65	0.28
Arg2D-Ala	bp1-D-Ala2	>25	nd	nd
Ala3D-Ala	bp1-D-Ala3	>25	nd	nd
Ala3Lys	bp1-110	1.9	nd	nd
Gly4D-Ala	bp1-D-Ala4	1.2	1.23	0.16
Pro5Arg	bp1-131	4.8	nd	nd
Pro5Asn	bp1-134	3.4	0.86	0.07
Pro5Thr	bp1-133	1.7	1.07	0.08
Trp8βNap	bp1-123	4.8	1.21[e]	0.18[e]
Trp8His	bp1-124	3.8	0.80	0.10
Trp8Arg	bp1-122	3.3	nd	nd
Leu6Nle	bp1-136	6.2	1.23	0.24
Leu6Arg	bp1-132	>40	0.99	0.08
Leu9Nle	bp1-137	1.9	1.23	0.27
Leu9Arg	bp1-126	>40	0.77	0.08
Tyr13Phe	bp1-68	5.3	nd	nd
Tyr13Aib	bp1-Aib13	6.3	nd	nd
Phe14Tyr	bp1-*xx*	3.5	nd	nd
Tyr13Ala/Phe14Ala	bp1-118	23.0	1.55	0.16
Δ15	bp1-116	0.89	1.49	0.28
Δ13−15	bp1-117	31.0	1.19	0.15
Δ12−15	bp1-04	>200	1.35	0.13

[a] βNap, β-naphthylalanine; Aib, aminoisobutyric acid; Nle, norleucine. [b] Relative inhibitory activities were determined from the IC_{50} for inhibition of IGFBP-1 binding to immobilized IGF-I in BIAcore competition assays; the inhibition by the analogue peptide [IC_{50}(mut)] is compared to the inhibition by bp1-01 [IC_{50}(wt) = 1.1 ± 0.7 μM]. [c] The rms differences of $^3J_{HN-H\alpha}$ between the analogue listed at the left and the unfolded cysteine to serine analogue (bp1-06). NMR data were not analyzed for the analogues indicated by nd. [d] The rms differences in H^α chemical shift between the analogue listed at the left and the unfolded cysteine to serine analogue (bp1-06). NMR data were not analyzed for the analogues indicated by nd. [e] NMR data collected in 10% (v/v) d_3-acetonitrile to limit self-association of this peptide.

siderations and steric interactions between the side chain and the ring of Pro5. This is found experimentally, as the Gly4 to L-Ala substitution was very detrimental to both the activity (50-fold effect on IC_{50}) and structure of bp1-01. Analysis of NMR spectra for this analogue indicated the presence of two species arising from cis−trans isomerization of the Ala4−Pro5 peptide bond with the predominant trans isoform (~70%) having a perturbed structure (Table 1). However, replacing Gly4 with D-Ala (Table 2) results in a peptide that adopts a single conformation similar to that of bp1-01 and has activity equivalent to that of bp1-01. Thus, a positive ϕ angle is necessary at position 4 for tight binding. Replacement of the adjacent proline residue with arginine or the more common helix N-cap residues asparagine and threonine decreased the level of inhibition by only 2−5-fold. The structure determined previously for bp1-01 indicated that the helix is capped by an unusual motif in which the indole hydrogen of Trp8 forms a hydrogen bond to the carbonyl oxygen of Pro5 (*5*). The hydrophobic bulk of the tryptophan and this hydrogen bond interaction both appear to be important for activity since replacing Trp8 with histidine (presumably allowing the hydrogen bond) and replacing Trp8 with β-naphthylalanine (hydrophobic bulk similar to that of tryptophan) both reduced the level of binding slightly (Table 2).

Leu6 and Leu9 were completely conserved in the polyvalent display phage selection experiments (Figure 1 and Table 2 of the Supporting Information) and were very sensitive to alanine substitution (Table 1). Analogues with each Leu replaced with Arg were prepared in an attempt to preserve the hydrophobic interactions between the side chains in the helix (i.e., preserve the structure of bp1-01) while presenting a polar exterior face that might interfere with IGFBP-1 binding. These analogues did not bind but were only partially folded, suggesting that the increase in IC_{50} may be due to a structural perturbation of the helix. Finally, the leucines were replaced with the non-natural amino acid norleucine. NMR data indicated that these analogues were folded (Table 2), while BIAcore measurements showed only a 6-fold (Leu6) or 2-fold (Leu9) increase in IC_{50}. Thus, aliphatic side chains are required in the central stripe of the helix to promote structure and efficient binding to IGFBP-1.

In the C-terminal region, removal of the phenolic hydroxyl of Tyr13 increased the IC_{50} by 5-fold (bp1-68; Table 2), whereas replacing both Tyr13 and Phe14 with alanine resulted in a 23-fold reduction (bp1-118; Table-2). C-Terminal truncations were also deleterious to binding, giving rise to a 31- or >200-fold increase in IC_{50} with removal of Tyr13−Gly15 (bp1-117) or Lys12−Gly15 (bp1-04), respectively. An ensemble of structures was calculated on the basis of the NMR data for the latter peptide. As depicted in Figure 3, bp1-04 contains a single turn of helix (Leu6−Glu11), a type I reverse turn (Gly4−Pro5), and a relatively ill-defined loop (Cys1−Gly4). All of these features are present in bp1-01, giving rise to an rmsd between bp1-04 and bp1-01 of 0.54 Å (calculated using backbone atoms of residues 1−10 in the mean structures). Thus, the C-terminus of bp1-01 is required for binding to IGFBP-1 but is not necessary for the rest of the peptide to fold.

Alternative Presentation of the bp1-01 Helix. A scaffold that remains helical even when the central hydrophobic residues are substituted would allow deconvolution of

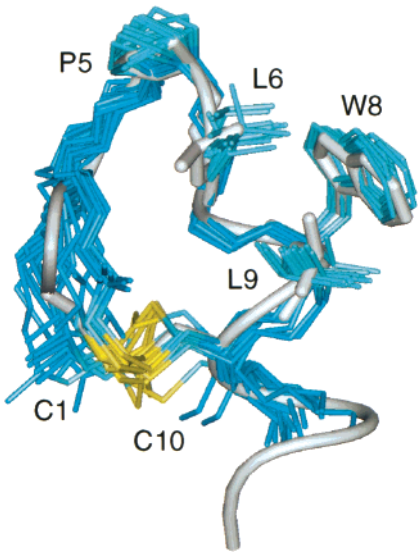

FIGURE 3: C-Terminal truncation of bp1-01. The ensemble of 20 structures for bp1-04 (blue) is overlaid on the minimized mean structure of bp1-01 (white) using the N, C^{α}, and C atoms of residues Pro5−Cys10. For clarity, only side chain heavy atoms of Cys1, Pro5, Leu6, Trp8, Leu9, and Cys10 are shown. This figure was prepared using the program InsightII (MSI, San Diego).

structural destabilization from direct IGFBP-1 contact effects on IC_{50}. Previous studies have shown that side chains of residues at *i* and *i* + 7 are sufficiently close in a helix (∼10 Å) that creating a covalent tether between them stabilizes a helical conformation (*22*). A suitable cross-linking chemistry involves replacement of the two residues with glutamates that are coupled via amide bonds with 1,5-diaminopentane. The preceding structure−activity data indicate that only the hydrophobic face is required for binding and therefore a covalent tether could be introduced on the nonhydrophobic face of bp1-01. Moreover, due to the nonclassical nature of the C-terminus of the bp1-01 helix, C^{α} of Gln7 is ∼10 Å from both Phe14 C^{α} (*i* + 7) and Gly15 C^{α} (*i* + 8). Hence, a series of locked-helix analogues were synthesized that lacked the disulfide bond but contained a tether linking position 7 to either position 14 or 15. A further benefit of the locked-helix scaffold is that N-terminal truncation may be performed since residues 1−6 are outside the constraining macrocycle. BIAcore competition assays and NMR data were collected on the peptides to assess binding to IGFBP-1 and the structural integrity of the peptides (Table 3).

Presentation of Leu6−Tyr13 in a locked-helix framework with either the *i*−*i* + 7 or *i*−*i* + 8 tether does not produce peptides capable of binding to IGFBP-1. However, NMR parameters for these analogues do not provide any evidence of helical structure; in addition to the coupling constant and chemical shift data summarized in Table 3, none of the medium-range NOEs expected for a helix were observed. The influence of the N-terminus on structure and binding was tested by the addition of N-terminal residues to the constrained core of the locked-helix peptides. Addition of an N-terminal proline led to *i*−*i* + 7 or *i*−*i* + 8 peptides that were only 20- or 3-fold reduced in affinity relative to bp1-01, respectively. Inclusion of additional residues N-terminal to the proline resulted in a peptide that was only 8-fold reduced in its level of binding for the *i*−*i* + 7 case. For these tight binding peptides, a well-folded helix is apparent from the coupling constant and chemical shift data summarized in Table 3. Moreover, many *i*−*i* + 3 H^{α}−H^{N} or H^{α}−H^{β} NOEs were observed for these peptides, confirming a helical structure. We presume that the covalent tether kinetically traps the helical conformation as the lock is closed on the resin. The data presented here suggest that in the absence of residues N-terminal to Leu6, either the helix is not highly populated prior to formation of the final macrocyclic bond or the small N-terminus of the peptide can feed through the macrocycle and unwind the helical structure. Nonetheless, once additional N-terminal residues are included, a stable helical structure is produced.

For two of the potent helical peptides [bp1(*i* + 7)C and bp1(*i* + 8)D], restraints were generated from the NMR data and used to determine structures; in both cases, the backbone atoms within the helix are well-defined (mean backbone atom rmsds from the mean structures are 0.18 ± 0.06 Å for Pro5−Gln14 of the *i*−*i* + 7 peptide and 0.38 ± 0.11 Å for Pro5−Gln15 of the *i*−*i* + 8 peptide), as are the hydrophobic side chains. The *i*−*i* + 7 variant has a backbone conformation similar to that of bp1-01 (mean backbone atom rmsd from the mean bp1-01 structure of 1.11 ± 0.04 Å for residues 5−14), although some of the side chain orientations are perturbed, presumably due to replacement of Phe14 with the tether (Figure 4A). The *i*−*i* + 8 variant is very similar to bp1-01 at both the backbone (mean backbone atom rmsd from the mean bp1-01 structure of 0.62 ± 0.08 Å for residues 5−15) and side chain level (Figure 4B).

Alanine substitutions of Leu9 made in the context of the locked-helix scaffolds lead to a greater than 200-fold reduction in the level of inhibition compared to bp1-01. In the case of the *i*−*i* + 7 scaffold, the NMR parameters indicate that the helix is still highly populated (Table 3). Thus, the decrease in the level of inhibition can be attributed directly to a contact between Leu9 and IGFBP-1. Curiously, the NMR parameters for the alanine-containing *i*−*i* + 8 scaffold suggest that the helix is not significantly populated (Table 3). Thus, the *i*−*i* + 8 scaffold mimics bp1-01 very closely, in that it has a well-folded helix when residue 9 is a leucine, but is not folded when this residue is substituted with alanine. Presumably, the extra residue between the tethering points in the *i*−*i* + 8 molecule allows a greater degree of conformational variability than in the *i*−*i* + 7 case.

Molecular Surface of bp1-01. Analysis of the bp1-01 ensemble reveals that in 15 of the 20 structures there is a small cavity adjacent to the hydrophobic surface of the helix (Figure 5A). The side chains of Leu6, Leu9, and Phe14 define the sides of this feature, and the side chain of Cys10 forms the bottom. The N-terminal residues of bp1−01 are the least well-defined part of the structure; hence, in five cases, the side chains of Cys1 or Ala2 partially occlude the opening. This pocket is about the size of a methyl group, and potentially represents a binding site for some (as yet unspecified) protrusion on the surface of IGFBP-1. To test whether this feature is important for IGFBP-1 binding, four peptide analogues were prepared with the aim of filling this hole by the addition of atoms to the aromatic ring of Phe14 (4-methyl, 3-methoxy, 4-hydroxy-3-iodo, or 4-hydroxy-3,5-diiodo). All analogues had activities lower than that of bp1-01 (Table 4). NMR data collected on the 4-methyl and 3-methoxy variants indicate that the overall bp1-01 fold is maintained, and that intense ROE peaks were observed

Table 3: Relative Activities of bp1-01 Locked-Helix Variants

analogue	sequence[a]	relative activity[b] IC_{50}(mut)/IC_{50}(wt)	$^3J_{HN\text{-}H\alpha}$[c] (Hz)	$\delta(H^\alpha)$[d] (ppm)
bp1-01	CRAGPLQWLCEKYFG	1.0	1.65	0.28
bp1(i + 7)A	ac-LXWLAEKYXG	>360	0.80	0.09
bp1(i + 7)B	ac-PLXWLAEKYXG	20	1.46	0.15
bp1(i + 7)C	ac-RAGPLXWLAEKYXG	7.7	1.95	0.18
bp1(i + 7)D	ac-RAGPLXW**A**AEKYXG	>200	1.75	0.09
bp1(i + 8)A	ac-LXWLAEKYFX	>200	n.d.	n.d.
bp1(i + 8)B	ac-PLXWLAEKYFX	2.8[g]	1.16[e]	0.19[e]
bp1(i + 8)C	ac-GPLXWLAEKYFX	3.1[g]	1.29[f]	0.19[f]
bp1(i + 8)D	ac-RPLXWLAEKYFX	7.7	1.37	0.17
bp1(i + 8)E	ac-AGPLXWLAEKYFX	2.8[g]	1.04[e]	0.12[e]
bp1(i + 8)F	ac-RAGPLXWLAEKYFX	5.9	n.d.	n.d.
bp1(i + 8)G	ac-RAGPLXW**A**AEKYFX	>200	0.59	0.09

[a] X indicates the glutamate residues connected via the 1,5-diaminopentane linker. [b] Relative inhibitory activities were determined from the IC_{50} for inhibition of IGFBP-1 binding to immobilized IGF-I in BIAcore competition assays; the inhibition by the analogue peptide [IC_{50}(mut)] is compared to the inhibition by bp1-01 [IC_{50}(wt) = 1.1 ± 0.7 μM]. [c] The rms differences of $^3J_{HN-H\alpha}$ between the analogue listed at the left and the unfolded cysteine to serine analogue (bp1-06); "unfolded" coupling constants for the linker residues and Ala10 (previously cysteine) were taken from Gln7 or Ala3 in bp1-06. NMR data were not analyzed for the analogues indicated by nd. [d] The rms differences in H^α chemical shift between the analogue listed at the left and the unfolded cysteine to serine analogue (bp1-06); "unfolded" chemical shifts for the linker residues and Ala10 (previously cysteine) were taken from Gln7 or Ala3 in bp1-06. NMR data were not analyzed for the analogues indicated by nd. [e] NMR data were collected in the presence of 10−15% (v/v) d_3-acetonitrile to limit self-association of the peptide. [f] NMR data collected at pH 3.0 due to precipitation at pH >3.5. [g] Activity determined in 2.5% DMSO because of limited peptide solubility. The relative activity is compared to that of bp1-01 under these conditions [IC_{50}(bp1-01) = 5.5 ± 0.2 μM].

between the newly introduced methyl group and side chain atoms of Leu9 and Leu6 (Figure 5). The most likely explanation for these data is that the additional substituents partially or completely fill the surface cavity on bp1-01 and, as a result, perturb binding to IGFBP-1. However, we note that the extra atoms are proximal to important IGFBP-1-binding residues Leu6 and Leu9; hence, the decrease in the level of binding may also be due to some perturbation of the surface of bp1-01 in this region other than filling the cavity.

Surface Similarity of bp1-01 and IGF-I. Primary and secondary structure comparisons between IGF-I and bp1-01 failed to produce a common sequence that might be an epitope for IGFBP-1 binding. However, the phage-derived peptides are able to compete with IGF-I for binding to IGFBP-1, and presumably, bp1-01 and IGF-I have partially overlapping binding sites on the binding protein. Thus, bp1-01 likely mimics some portion of the surface of IGF-I. Mutagenesis of IGF-I has recently identified the side chains of Glu3, Leu10, Phe25, and Phe49 as having a >20-fold reduced level of binding to IGFBP-1 when replaced with alanine (*16*). The latter three residues form part of a surface-exposed hydrophobic patch that also includes Val11, Leu14, and Val44 [using the minimized mean structure of Cooke et al. (*26*)], and likely constitutes the IGFBP-1 binding surface. We hypothesize that the hydrophobic patch on bp1-01 mimics this surface of IGF-1 when it binds to IGFBP-1. On the basis of this analysis, IGF-I and bp1-01 were manually superimposed so as to overlay in three dimensions the important side chains of bp1-01 with some of the IGF-I side chains implicated in binding to IGFBP-1 (Phe14 with Phe25 of IGF-I, Leu6 with Val11 of IGF-I, Leu9 with Leu10 of IGF-I, and Tyr13 with Val44 of IGF-I; see Figure 6A). The important IGF-I residues, Glu3 and Phe49, are not mimicked by bp1-01 in this model; these additional contacts by IGF-I may explain its 100−1000-fold tighter binding affinity for IGFBP-1. However, this overlay does show how the short sequence of bp1-01 can mimic several residues from different regions of IGF-I that are not close in sequence but are close in space.

Although a number of structures have been published for IGF-1 and its variants (*26*−*29*), they are all ill-defined due to the poor quality of the NMR spectra. The low spectral quality has been attributed to a combination of self-association and conformational exchange broadening (*26*, *30*, *31*), and the dynamic nature of the protein has been investigated by heteronuclear relaxation experiments (*28*). Although there is variation in the exact orientation of the side chains of IGF-I within and among these NMR ensembles, in all cases the hydrophobic residues described above do form a solvent accessible patch. Moreover, in the minimized mean structure determined by Cooke et al. (*26*), the molecular surfaces of IGF-I and bp1-01 have similar shapes in this region (including the cavity described above for bp1-01; Figures 5 and 6), suggesting that they may bind to a common site on IGFBP-1. The poor definition of IGF-I structures precludes us from making more detailed predictions about the importance of this cavity for IGF-I binding

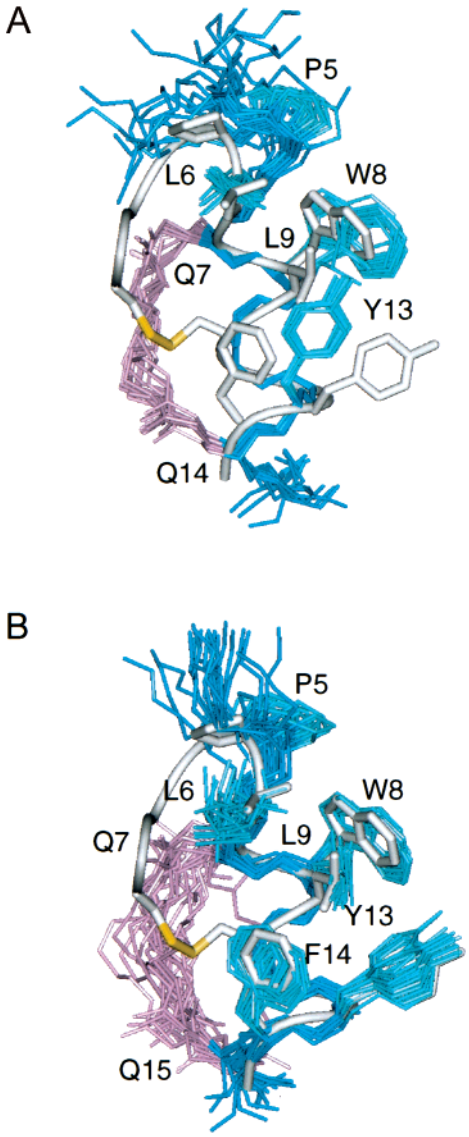

FIGURE 4: Structural comparison of locked-helix peptides with bp1-01. (A) Ensemble of 20 structures for the locked-helix peptide bp1-(i + 7)C (blue) are overlaid on the minimized mean bp1-01 structure (white) using the N, C^{α}, and C atoms of residues Gln7−Phe14. The side chain heavy atoms of Glu7 and Glu14 and the amide linker of the locked helix are colored pink. (B) Ensemble of 20 structures for the locked-helix peptide bp1(i + 8)D (blue) are overlaid on the minimized mean bp1-01 structure (white) using the N, C^{α}, and C atoms of residues Gln7−Gly15. The side chain heavy atoms of Glu7 and Glu15 and the amide linker of the locked helix are colored pink. This figure was prepared using the program InsightII (MSI, San Diego).

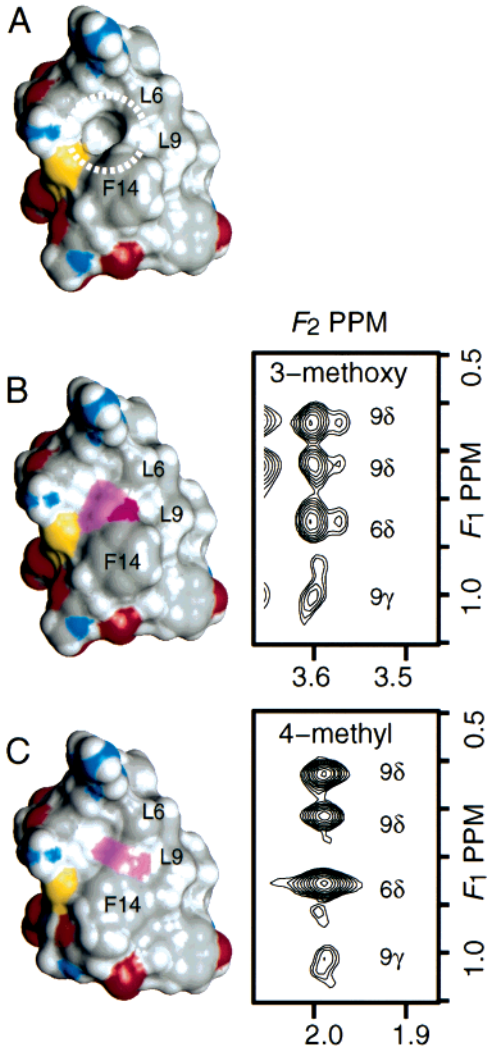

FIGURE 5: Analogues of bp1-01 lacking the surface cavity. (A) Surface representation of the minimized mean bp1-01 structure with the obvious cavity seen above the Phe14 side chain. The surface pocket is denoted by the dotted line. Atoms are color coded according to atom type. (B) Modeled structure of analogue with 3-methoxy Phe14; the additional methoxy group is colored pink. At right is a section of the ROESY spectrum showing the ROEs from the methoxy methyl group at 3.60 ppm to the side chains of Leu6 and Leu9 justifying the location of the methoxy group in the modeled structure. (C) Modeled structure of analogue with 4-methyl Phe14; the additional methyl group is colored pink. At right is a section of the ROESY spectrum showing the ROEs from the methyl group at 1.98 ppm to the side chains of Leu6 and Leu9 justifying the location of the methyl group in the modeled structure. This figure was prepared using the program InsightII (MSI, San Diego).

and the exact shape of the IGF-I surface when bound to IGFBP-1.

DISCUSSION

A growing body of work suggests that phage display of naïve peptide libraries is a reliable way of generating peptides that bind to a wide range of protein targets (*17*). Moreover, these ligands often bind in a manner that modulates biological function, for example, by blocking protein−protein interaction surfaces (*3*, *8*−*10*) or interfering with the catalytic processes of an enzyme (*7*). Molecules having these characteristics hold great potential as drug candidates in cases where specific protein−protein interactions or enzyme activities are the causative agent for a particular disease state. However, unless some means of delivery to a target site within cells, tissues, or the vasculature can be established [e.g., by injection into the bloodstream or coupling with an agent that will be actively transported across membranes (*32*)], peptides are not usually considered as readily bioavailable drug candidates. Since the phage-derived peptides presumably bind to their targets using a covalent arrangement of amino acids that is distinct from the natural ligands or substrates, these peptides do provide new insights into how binding can be achieved. Understanding the details of the interaction can potentially lead to the design of novel, small

Table 4: Affinities for bp1-01 Hole-Filled Analogues

	relative activity[a] IC_{50}(mut)/IC_{50}(wt)	$^3J_{HN-H\alpha}$[b] (Hz)	$\delta(H^\alpha)$[c] (ppm)
wild type	1.0	1.65	0.28
4-methyl Phe14	22.8	1.74	0.27
3-methoxy Phe14	7.2	1.59	0.24
4-hydroxy-3-iodo Phe14	7.0[d]	nd	nd
4-hydroxy-3,5-diiodo Phe14	21.3[d]	nd[e]	0.24[e]

[a] Relative inhibitory activities were determined from the IC_{50} for inhibition of IGFBP-1 binding to immobilized IGF-I in BIAcore competition assays; the inhibition by the analogue peptide [IC_{50}(mut)] is compared to the inhibition by bp1-01 [IC_{50}(wt) = 1.1 ± 0.7 μM]. [b] The rms differences of $^3J_{HN-H\alpha}$ between the analogue listed at the left and the unfolded cysteine to serine analogue (bp1-06). NMR data were not analyzed for the analogues indicated by nd. [c] The rms differences in H^α chemical shift between the analogue listed at the left and the unfolded cysteine to serine analogue (bp1-06). NMR data were not analyzed for the analogues indicated by nd. [d] Assay performed with 1% DMSO to limit self-association of the iodotyrosine peptides. The relative activity is compared to that of bp1-01 under these conditions (IC_{50} = 5.5 ± 0.2 μM). [e] NMR data were collected in the presence of 15% (v/v) d_3-acetonitrile to limit self-association of the peptide; due to line widths and low concentration, $^3J_{HN-H\alpha}$ could not be measured accurately.

organic molecules that bind in a fashion similar to that of the peptide but show more favorable oral bioavailability characteristics.

Structural analysis must play a key role in understanding the arrangement of atoms in the phage-derived peptide that recognizes a target protein. This can be most readily accomplished by an experimental determination of a peptide−protein complex structure; such data cannot always be obtained readily. Although peptides of fewer than 20 residues rarely adopt stable, compact folds, our studies indicate that the phage optimization process not only results in tight binding but also often produces peptides that are highly structured when free in solution (*5*, *7*). Such cases provide a structural framework in which structure−activity data may be rationalized.

The current studies focus on inhibiting the interaction between IGF-I and IGFBP-1. Thus far, the latter has not been amenable to structural characterization by X-ray crystallography or NMR methods. As a further complication, the natural ligands to IGFBP-1 (IGF-I and IGF-II) do not provide a good starting point for structure-based design of antagonists as their structures are poorly defined by the available NMR data (*26*−*28*), and they may also change conformation on binding (*30*). Thus, the study of phage-derived peptide inhibitors of the interaction provides a unique way of undertaking a structure-based design of small molecule antagonists. Since bp1-01 is highly structured, it provides a suitable starting point for the generation of a pharmacophore model.

The exposed hydrophobic surface of bp1-01 represents a likely binding site for IGFBP-1, and this hypothesis was given extra weight by the conservation of these residues in phage-randomization experiments (Figure 1A and Table 2 of the Supporting Information). Subsequent alanine-scan data indicated that the central leucine of this patch (Leu9) and the peripheral hydrophobic residues (Leu6, Trp8, Tyr13, and Phe14) all had a significant effect on IGFBP-1 binding when replaced (Table 1 and Figure 1B). Replacement of both cysteine residues with serine, C-terminal truncations, or

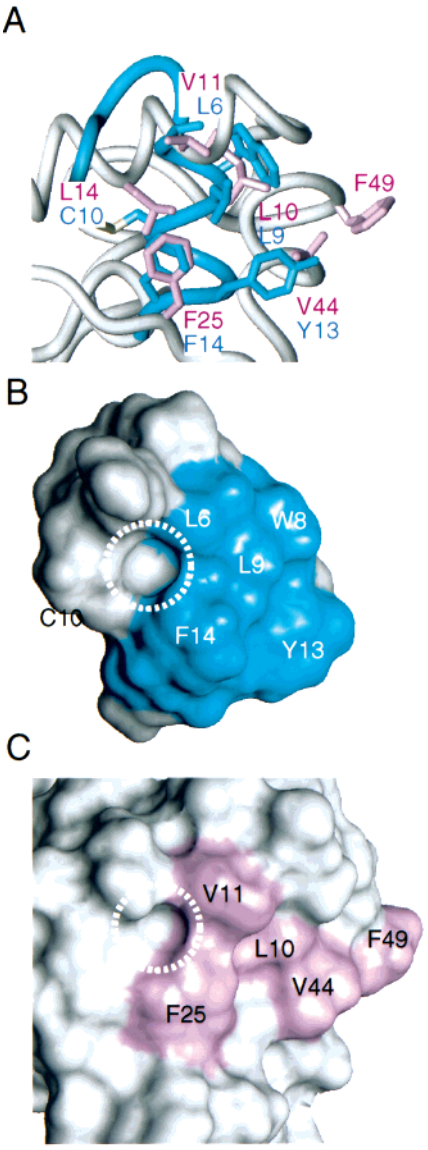

FIGURE 6: Comparison of the IGFBP-1 binding site on bp1-01 and IGF-I. (A) IGF-I (white tube and pink rods) is overlaid with bp1-01 (blue tube and rods) so as to superimpose a number of the side chains that are important for IGFBP-1 binding (see the text). The minimized mean structure of IGF-I was used [PDB accession number 2GF1 (*26*)]. (B) Surface representation of bp1-01 [minimized mean (*5*)] with the hydrophobic side chains that are important for binding colored blue. The common surface depression is between Leu6 and Phe14 and is denoted by the dotted line. (C) Surface representation of IGF-I (minimized mean structure from ref *26*) with the side chains that are most important for IGFBP-1 binding shown in pink (*16*). The important surface depression is between Phe25 and Val11 and is denoted by the dotted line. This figure was prepared using the program InsightII (MSI, San Diego).

replacement of Gly4 with alanine also leads to a dramatic loss of binding. However, additional substitutions in and around the turn (e.g., Pro5 to arginine, threonine, or asparagine; Trp8 to β-naphthylalanine or histidine) had only a modest effect on binding. In summary, the hydrophobic patch (including the C-terminal turn of helix), the disulfide bond, and some features of the turn prior to the helix are important determinants of IGFBP binding (Figure 7).

The reduced level of binding observed for these analogues does not necessarily indicate that the removed atoms should be included in a pharmacophore model; in addition to the

FIGURE 7: Summary of bp1-01 features that are important for IGFBP-1 binding. A helical scaffold (pink, stabilized by the disulfide bond and hydrophobic packing, or an $i-i+7$ or 8 covalent tether) presents a hydrophobic patch (Leu6 and Leu9, blue) surrounded by a layer of aromatic residues (light blue). A turn prior to the N-terminus of the helix is also required (green), and the backbone atoms at the C-terminus of the helix may contact IGFBP-1. This figure was prepared using the program InsightII (MSI, San Diego).

removal of a direct IGFBP-1 contact, the altered binding could result from a perturbation of the peptide conformation that is necessary for binding. To discriminate between these two possibilities, NMR data were analyzed for many of the analogues. Removal of the disulfide bond or replacing Gly4 with an L-amino acid led to poorly structured peptides, suggesting that the loss of helical structure affects binding rather than the loss of a direct contact. Replacement of the leucines led to a significant loss in structure, demonstrating that the helix is important, but direct contacts from the leucine side chains are not identified unequivocally from these data. Removal of the aromatic side chains does not perturb the structure of bp1-01 significantly; hence, the decrease in the level of binding of these analogues can be attributed to direct contacts with IGFBP-1. Deletion of the C-terminal tail of the helix (Lys12, Tyr13, Phe14, and Gly15) resulted in very poor inhibition (Table 3). However, NMR analysis of bp1-04 (Figure 3) indicates that C-terminal truncation does not affect the structure of the N-terminal portion of the peptide. Thus, "structural perturbation" caused by the C-terminal deletion does not appear to be playing a role, and the loss of favorable interactions between IGFBP-1 and the C-terminal residues of the helix explain the inhibition data.

This analysis highlights that in addition to the disulfide bond, hydrophobic interactions play a crucial role in stabilizing the compact fold observed in the selected peptide. Such intrapeptide hydrophobic interactions were also important in the case of a phage-derived peptide that binds to FVIIa (*7*) and also appears to be important from the bound structures of peptides that recognize the erythropoietin receptor, an antibody Fc domain, or a portion of gp41 from HIV-1 (*3*, *9*, *10*). Such clusters of hydrophobic side chains may be a common feature of compact peptides derived from phage display libraries. Given the small size of these peptides, this inevitably means that some side chains will play a dual role by stabilizing the peptide conformation necessary for binding and by providing direct contacts to the target protein. Deconvolution of a pharmacophore model from peptide analogue data is not straightforward, and detailed structural analysis of many peptide analogues may be necessary for understanding these systems.

The generation of a pharmacophore model based on the structure of a free peptide assumes that the peptide does not alter its conformation significantly on binding. Even though the helical conformation of bp1-01 is maintained at temperatures exceeding 55 °C (*5*), the noncovalent interactions that stabilize the compact fold of bp1-01 could be disrupted on binding. To probe this, the side chains of the helix important for binding were transferred to an alternate scaffold that is less dependent on noncovalent interactions for stability. This scaffold utilizes a covalent tether between side chains at positions i and $i+7$ or $i+8$ in the helix that are ~10 Å apart in the original bp1-01 structure (*22*). Structures determined for two of these peptides demonstrate such a scaffold enforces a conformation that is very similar to bp1-01 at both the backbone and side chain level, particularly for the $i-i+8$ version (Figure 4). Moreover, the locked-helix peptides are able to bind to IGFBP-1 nearly as tightly as bp1-01 (Table 3). Given the constrained nature of the tether, conformational reorganization of the helix on binding to IGFBP-1 is unlikely; hence, the presentation of the hydrophobic side chains from a helical backbone conformation is necessary for these peptides to bind to IGFBP-1, and this conformation is preserved in the bound state.

Moving to the locked-helix scaffold allows reduction of the peptide size via N-terminal truncation (this is precluded in bp1-01 due to the N-terminal cysteine residue). In the case of the bp1-01 mimics, two or more residues are required N-terminal to the constrained portion for a folded, helical conformation to predominate. The truncation series reported in Table 3 indicates that potent molecules are obtained with three residues N-terminal of the constrained portion, but adding more than three residues does not improve the affinity. Since the structure of the $i-i+7$ locked-helix scaffold does not depend on noncovalent interactions within the macrocyclic portion of the molecule, the importance of side chains within the helix can be evaluated. For example, replacement of Leu9 with alanine in the locked-helix context results in a >200-fold decrease in the level of binding (Table 3); NMR analysis of this peptide indicates that the helical structure is preserved in the $i-i+7$ case. Taken together, these two observations imply that the side chain atoms of Leu9 do make direct contacts with IGFBP-1. Thus, moving to an alternate scaffold that is more rigid not only tests our understanding of the arrangement of side chains in the bound state but also allows discrimination between structural and direct contact effects on binding.

Previously, analysis of structure−activity data has allowed the successful transfer of epitopes from small cyclic peptides (six to eight residues) of nonphage origin to organic molecules either by design (e.g., see refs *33*−*37*) or by screening focused combinatorial libraries (*38*−*40*). Although bp1-01 is highly structured and selective for human IGFBP-1 (bp1-01 does not bind to other human IGF binding proteins or to the ~70% identical rat IGFBP-1), this peptide is significantly larger than the peptides that have previously been "minimized" in this fashion. Transfer to the locked-helix scaffold allows N-terminal truncation to an 11-residue

peptide, in the case of bp1($i-i+8$)B, that has activity within 3-fold of that of the 15-residue parent. However, the main elements of the pharmacophore model described in Figure 7 are still spread over two turns of helix and occupy an area of ~10 Å × ~12 Å. Moreover, the interactions are predominantly hydrophobic in nature (even allowing for the possibility of polar interactions with the carbonyl oxygen atoms in the C-terminal turn of helix of bp1-01). Thus, designing an organic scaffold to display such an epitope while retaining solubility in aqueous buffers presents a significant challenge.

A key feature of phage-derived peptides is that their primary sequence is distinct from that of endogenous ligands. However, the peptides often compete for binding with the native protein, and hence in some way mimic the presentation of atoms within the native ligand (*9*). A detailed mutational analysis of IGF-I has recently identified the surface regions responsible for IGFBP-1 binding (*16*). The binding surfaces on IGF-I and bp1-01 are both predominantly hydrophobic in nature, and we hypothesize that they recognize the same region of IGFBP-1. Alignment of IGF-I and bp1-01 so as to overlap the hydrophobic side chains reveals a similarity in surface shape and suggests how the peptide is able to mimic the surface of IGF-I (Figure 6). Interestingly, in the modeled superposition of the common binding surfaces (Figure 6), the helix of bp1-01 does not coincide with any of the IGF-I helices, yet the peptide is able to produce a surface with features similar to those of the protein.

In conclusion, we have used a combination of phage selection, peptide synthesis, structural characterization, and molecular modeling to investigate the manner in which the phage-derived peptide bp1-01 recognizes IGFBP-1. The highly structured nature of the initial phage-derived peptide provides a framework for understanding details of the interaction with IGFBP-1, even in the absence of a complex structure (Figure 7). Due to the compact, hydrophobic nature of the bp1-01 fold, structural characterization of peptide analogues was crucial for identifying direct contacts with IGFBP-1. Presentation of the binding residues in a more rigid context confirms that structural features observed in the original phage-derived peptide are present in the bound state. These data are invaluable in evaluating whether the peptide-binding site on IGFBP-1 is amenable to targeting via a small molecule drug. The approach of using structure−activity data on a structured, phage-derived ligand might be a generally useful way of discovering and optimizing molecules of biological interest, even in cases where the receptor (or endogenous ligand) is not amenable to structural characterization. We note that small, compact clusters of hydrophobic residues have been observed at the binding interface of several phage-derived peptides (*3*, *7*, *8*, *10*); hence, the deconvolution of structural effects from receptor contacts is likely to be a recurring issue. Nonetheless, these studies demonstrate that this approach does hold promise in understanding molecular interactions of pharmaceutical interest.

ACKNOWLEDGMENT

We are grateful to Dr. Andrew Braisted for many helpful discussions concerning the preparation of the locked-helix peptides and for providing the FMOC-protected amino acid used in their synthesis. We also thank Dr. Robert McDowell for many interesting discussions at the outset of this work.

SUPPORTING INFORMATION AVAILABLE

Tables describing (1) details of the structure calculations (number of restraints, quality, and precision of the resulting structures), (2) the degree of conservation of residues in phage randomization experiments, and (3) ^{1}H chemical shift assignments and scalar coupling measurements for the peptides whose structures were calculated. This material is available free of charge via the Internet at http://pubs.acs.org.

REFERENCES

1. Lowman, H. (1997) *Annu. Rev. Biophys. Biomol. Struct. 26*, 401−424.
2. Sidhu, S. S., Lowman, H. B., Cunningham, B. C., and Wells, J. A. (2000) *Methods Enzymol. 328*, 333−363.
3. Livnah, O., Stura, E. A., Johnson, D. L., Middleton, S. A., Mulcahy, L. S., Wrighton, N. C., Dower, W. J., Jolliffe, L. K., and Wilson, I. A. (1996) *Science 273*, 464−471.
4. Fairbrother, W. J., Christinger, H. C., Cochran, A. G., Fuh, G., Keenan, C. J., Quan, C., Shriver, S. K., Tom, J. Y., Wells, J. A., and Cunningham, B. C. (1998) *Biochemistry 37*, 17754−17764.
5. Lowman, H. B., Chen, Y. M., Skelton, N. J., Mortensen, D. L., Tomlinson, E. E., Sadick, M. D., Robinson, I. C. A., and Clark, R. G. (1998) *Biochemistry 37*, 8870−8878.
6. Katz, B. A. (1997) *Annu. Rev. Biophys. Biomol. Struct. 26*, 27−45.
7. Dennis, M. S., Eigenbrot, C., Skelton, N. J., Ultsch, M. H., Santall, L., Dwyer, M. A., O'Connell, M. P., and Lazarus, R. A. (2000) *Nature 404*, 465−470.
8. Wiesmann, C., Christinger, H. C., Cochran, A. G., Cunningham, B. C., Fairbother, W. J., Keenan, C. J., Meng, G., and de Vos, A. M. (1998) *Biochemistry 37*, 17765−17772.
9. DeLano, W. L., Ultsch, M. H., de Vos, A. M., and Wells, J. A. (2000) *Science 287*, 1279−1283.
10. Eckert, D. M., Malashkevich, V. N., Long, L. H., Carr, P. A., and Kim, P. S. (1999) *Cell 99*, 103−115.
11. Katz, B. A. (1995) *Biochemistry 34*, 15421−15429.
12. Ullrich, A., Gray, A., Tam, A. W., Yang-Feng, T., Tsubokawa, M., Collins, C., Henzel, W., LeBon, T., Kathuria, S., Chen, E., Jacobs, S., Francke, U., Ramachandran, J., and Fuita-Yamaguchi, Y. (1986) *EMBO J. 5*, 2503−2512.
13. Baxter, R. C. (2000) *Am. J. Physiol.: Endocrinol. Metab. 278*, E967−E976.
14. Bondy, A., Underwood, L. E., Clemmons, D. R., Guler, H.-P., Bach, M. A., and Skarulis, M. (1994) *Ann. Int. Med. 120*, 593−601.
15. Kalus, W., Zweckstetter, M., Renner, C., Sanchez, Y., Georgescu, J., Grol, M., Demuth, D., Schumacher, R., Dony, C., Lang, K., and Holak, T. A. (1998) *EMBO J. 17*, 6558−6572.
16. Dubaquié, Y., and Lowman, H. B. (1999) *Biochemistry 38*, 6386−6396.
17. Lowman, H. B. (1998) in *Methods in Molecular Biology: Combinatorial Peptide Library Protocols* (Cabilly, S., Ed.) pp 249−264, Humana Press, Totowa, NJ.
18. Mortensen, L., Won, W. B., Siu, J., Reifsnyder, D., Gironella, M., Etcheverry, T., and Clark, R. G. (1997) *Endocrinology 138*, 2073−2080.
19. Löfås, S., and Johnsson, B. (1990) *J. Chem. Soc., Chem. Commun. 21*, 1526−1528.
20. Dubaquié, Y., Mortensen, D. L., Intintoli, A., Hogue, D. A., Nakamura, G., Rancatore, P., Lester, P., Sadick, M. D., Filvaroff, E., Fielder, P. J., and Lowman, H. B. (2001) *Endocrinology 142*, 165−173.
21. Peterman, J. H. (1991) in *Immunochemistry of solid-phase immunoassay* (Butler, J. E., Ed.) CRC Press, Boston.
22. Phelan, J. C., Skelton, N. J., Braisted, A. C., and McDowell, R. S. (1997) *J. Am. Chem. Soc. 119*, 455−460.

23. Cavanagh, J., Fairbrother, W. J., Palmer, A. G., and Skelton, N. J. (1995) *Protein NMR Spectroscopy, Principles and Practice*, Academic Press, New York.
24. Skelton, N. J., Garcia, K. C., Goeddel, D. V., Quan, C., and Burnier, J. P. (1994) *Biochemistry 33*, 13581−13592.
25. Havel, T. F. (1991) *Prog. Biophys. Mol. Biol. 56*, 43−78.
26. Cooke, R. M., Harvey, T. S., and Campbell, I. D. (1991) *Biochemistry 30*, 5484−5491.
27. Sato, A., Nishimura, S., Ohkubo, T., Kyogoku, Y., Koyama, S., Kobayashi, M., Yasuda, T., and Kobayashi, Y. (1993) *Int. J. Pept. Protein Res. 41*, 433−440.
28. Laajoki, L. G., Francis, G. L., Wallace, J. C., Carver, J. A., and Keniry, M. A. (2000) *J. Biol. Chem. 275*, 10009−10015.
29. De Wolf, E., Gill, R., Geddes, S., Pitts, J., Wollmer, A., and Grözinger, J. (1996) *Protein Sci. 5*, 2193−2202.
30. Jansson, M., Uhlen, M., and Nilsson, B. (1997) *Biochemistry 36*, 4108−4117.
31. Jansson, M., Andersson, G., Uhlén, M., Nilsson, B., and Kördel, J. (1998) *J. Biol. Chem. 273*, 24701−24707.
32. Prochiantz, A. (1996) *Curr. Opin. Neurobiol. 6*, 629−634.
33. McDowell, R. S., Blackburn, B. K., Gadek, T. R., McGee, L. R., Rawson, T., Reynolds, M. E., Robarge, K. D., Somers, T. C., Thorsett, E. D., Tischler, M., Webb, R. R. I., and Venuti, M. C. (1994) *J. Am. Chem. Soc. 116*, 5077−5083.
34. McDowell, R. S., Gadek, T. R., Barker, P. L., Burdick, D. J., Chan, K. S., Quan, C. L., Skelton, N., Struble, M., Thorsett, E. D., Tischler, M., Tom, J. Y. K., Webb, T. R., and Burnier, J. P. (1994) *J. Am. Chem. Soc. 116*, 5069−5076.
35. Hirschman, R., Nicolau, K. C., Pietranico, S., Leahy, S. M., Salvino, J., Arison, B., Cichy, M. A., Spoors, P. G., Shakespeare, W. C., Sprengler, P. A., Hamley, P., Smith, A. B. I., Reisine, T., Raynor, K., Maechler, L., Donaldson, C., Vale, W., Freidinger, R. M., Cascierie, M. R., and Strader, C. D. J. (1993) *J. Am. Chem. Soc. 115*, 12550.
36. Papageorgiou, C., Haltiner, R., Bruns, C., and Pletcher, T. J. (1992) *Bioorg. Med. Chem. Lett. 2*, 135.
37. Damour, D., Barreau, M., Blanchard, J.-C., Burgevin, M.-C., Doble, A., Herman, F., Pantel, G., James-Surcouf, E., Vuilhorgne, M., and Mignani, S. (1996) *Bioorg. Med. Chem. Lett. 6*, 1667−1672.
38. Ankersen, M., Crider, M., Liu, S., Ho, B., Andersen, H. S., and Stidsen, C. (1998) *J. Am. Chem. Soc. 120*, 1368−1373.
39. Yang, L., Guo, L., Paternak, A., Mosley, R., Rohrer, S., Birzin, E., Foor, F., Cheng, K., Schaeffer, J., and Patchett, A. A. (1998) *J. Med. Chem. 41*, 2175−2179.
40. Souers, A. J., Virgilio, A. A., Rosenquist, A., Fenuik, W., and Ellman, J. A. (1999) *J. Am. Chem. Soc. 121*, 1817−1825.

BI0103866